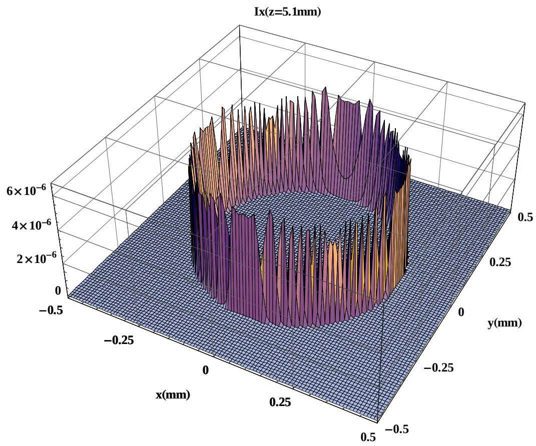

(a3) X polarization (Ix)
(z=5.10 mm)

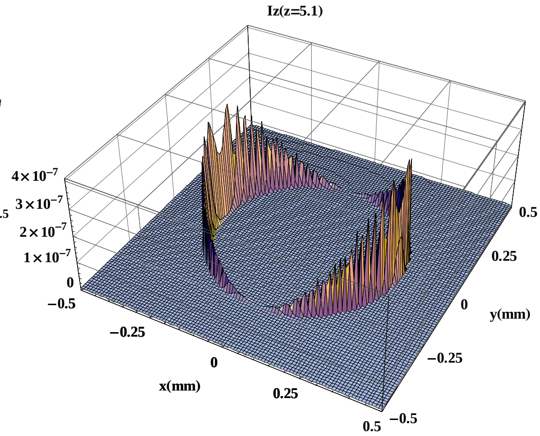

(b3) X polarization (Iz)
(z=5.10 mm)

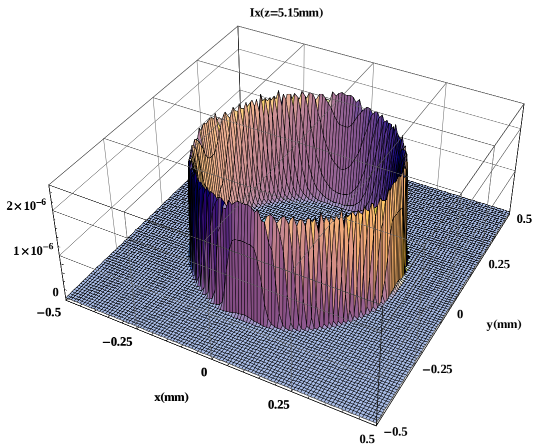

(a4) X polarization (Ix)
(z=5.15 mm)

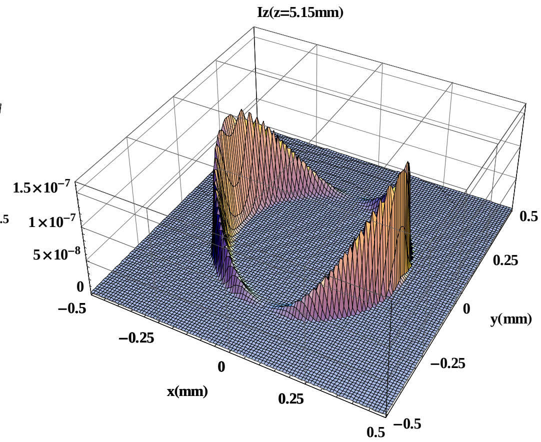

(b4) X polarization (Iz)
(z=5.15 mm)

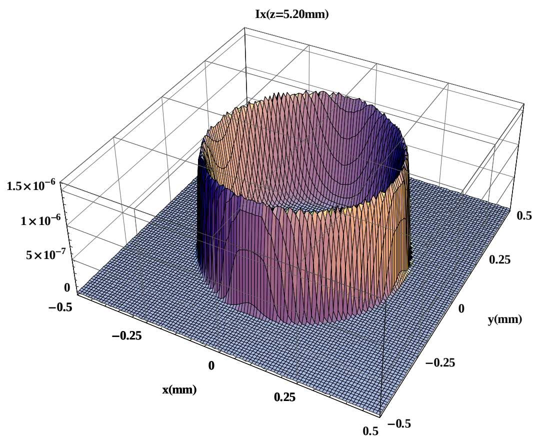

(a5) X polarization (Ix)
(z=5.20 mm)

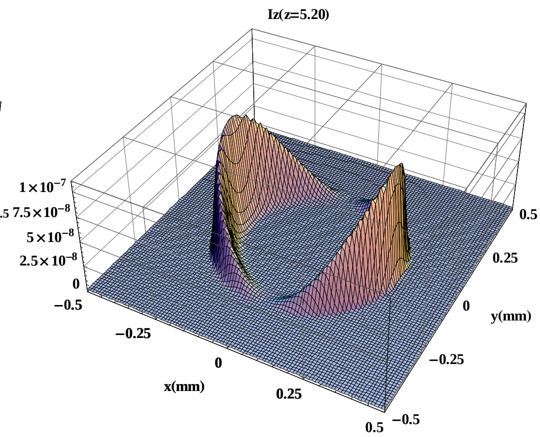

(b5) X polarization (Iz)
(z=5.20 mm)

Fig. 5.8 Cross sectional 3D beam profiles of x-polarization for $\gamma = 0.5^0$ and $f = 5.08$ mm at different position : (1) z = 4.95 mm; (2) z = 5.00 mm; (3) z = 5.10 mm; (4) z = 5.15 mm; (5) z = 5.20 mm.

In order to take a close look at the variation of the longitudinal field with change of γ and f, we plotted the radial profile across the peaks of 2D field distribution at z = Z_b in Figure 5.9 (a)~(d).

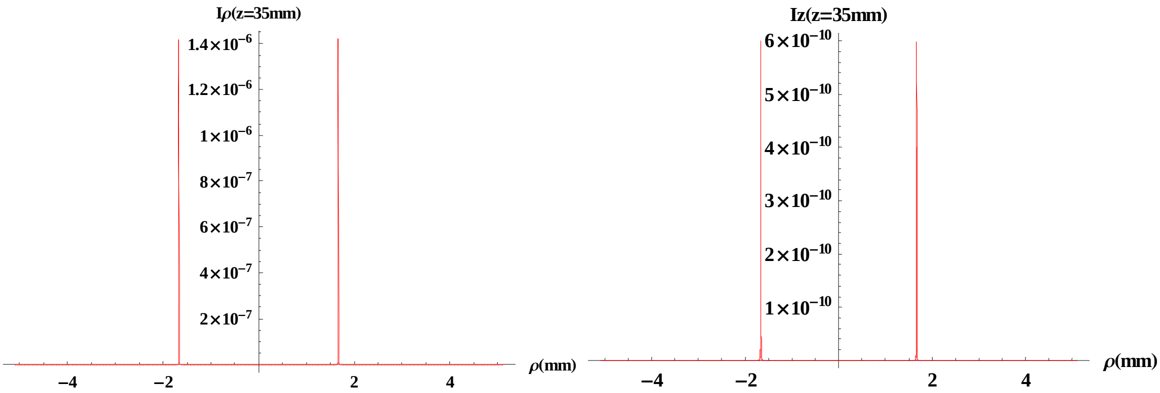

(a) gamma=5^0, f=35.08mm

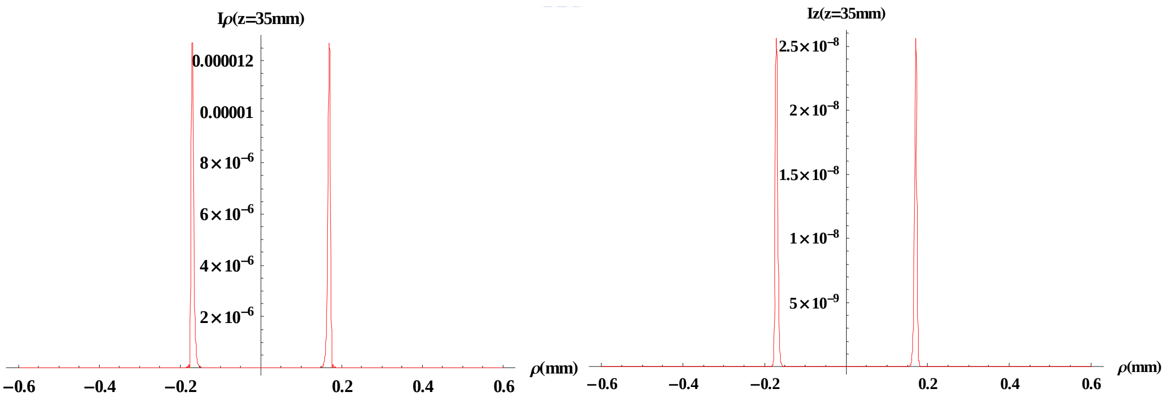

(b) gamma=0.5^0, f=35.08mm

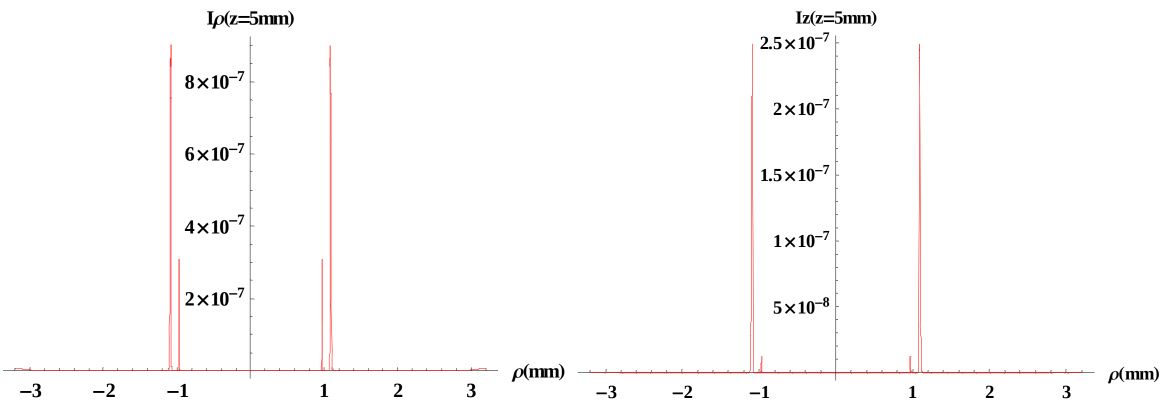

(c) gamma=5^0, f=5.08mm

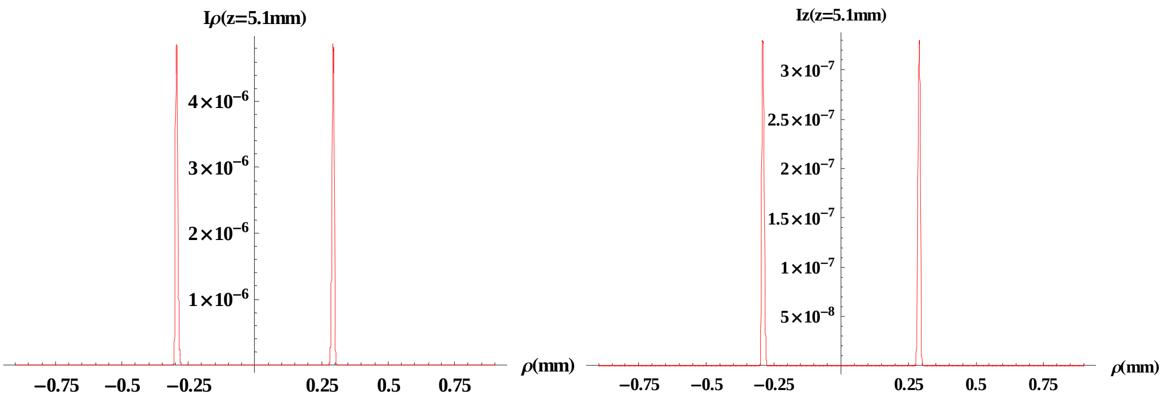

(d) gamma=0.5⁰, f=5.08mm

Fig. 5.9 Intensity comparisons of the traverse field (I_ρ) and the longitudinal field (I_z) at individual Z_b for various γ and f: (a) $\gamma = 5^0$ and $f = 35.08$ mm, (b) $\gamma = 0.5^0$ and $f = 35.08$ mm, (c) $\gamma = 5^0$ and $f = 5.08$ mm, and (d) $\gamma = 0.5^0$ and $f = 5.08$ mm.

Figure 5.8 (a) shows the result that the traverse field ($I_x + I_y$) is about three to four orders of magnitude much larger than the longitudinal field (I_z) with ring diameter of about 3.34 mm for $\gamma = 5^0$ and $f = 35.08$ mm. With reducing γ to 0.5°, Figure 5.8 (b) shows the ratio of I_z to ($I_x + I_y$) is still remained about three orders, but the ring diameter substantially decreases to 0.34 mm. The interesting result is for $\gamma = 5^0$ and $f = 5.08$ mm that I_z approaches to ($I_x + I_y$) in Figure 5.8 (c) with $I_z / (I_x + I_y) \sim 0.28$ and the ring diameter ~ 2.18 mm. Finally, we obtained $I_z / (I_x + I_y) \sim 0.08$ with ring diameter ~ 0.6 mm in Figure 5.8(d).

5.4 Discussion

In application of trapping of atoms and micro-sized particles, micrometer bottle range and ring diameter must be obtained in the laser trapping system. From Figure 5.8, the major effect of decreasing bottle range is to reduce the focal length of lens and the key point of decreasing ring diameter (D_b) is to use the smaller conical angle of axicon. From our simulation, we conclude reducing both focal length and conical angle of axicon is necessary for laser trapping of low-index microparticles.

Besides, the simulated position of the thinnest ring (Z_b) is close to the experiment no matter what radial or linear polarization light is used. The major difference of the linear polarization light is that the cross sectional patterns of the three polarizations depend on the observed angle β but the radial polarization one is cylindrical symmetry. The observed beam pattern of I_z that has two maximum points on the x-axis appeared as a function of $\cos^2\beta$. For this reason, the trapping force along the x-axis would be obviously larger than that along the y-axis if one uses small focal length of lens. Therefore, it would profit manipulating or rotating the elongated particles by rotating the polarization of linearly polarized input light field.